ARTICLE

OBC
www.rsc.org/obc

Trends in alkyl substituent effects on nucleophilic reactions of carbonyl compounds: Gas phase reactions between ammonia and $R^1R^2COCH_3^+$ oxonium ions †

Lihn Bache-Andreassen and Einar Uggerud *
Department of Chemistry, University of Oslo, P.O. Box 1033 Blindern, N-0315 Oslo, Norway. E-mail: einaru@kjemi.uio.no

Received 10th October 2002, Accepted 13th December 2002
First published as an Advance Article on the web 30th January 2003

The reactivity of carbonyl substituted methyl oxonium ions ($R^1R^2COCH_3^+$) towards ammonia has been investigated using an FT-ICR mass spectrometer and *ab initio* calculations. The monosubstituted ions (R^1=H; R^2= H, CH_3, C_2H_5 and *i*-C_3H_7) show different reaction patterns with variable degree of: (1) nucleophilic substitution, (2) addition–elimination and (3) proton transfer, when reacted with ammonia. In all cases addition–elimination dominates over nucleophilic substitution, and the observed reactions are slow. The trends in reactivity are consistent with the alkyl group's electronic properties, as expressed by a single parameter linear or slightly non-linear model.

Introduction

Oxonium ions ($R^1R^2COR^{3+}$) have been the subject of interest in several research groups during the last decades, in particular because of their ambident reactivity towards nucleophiles, but also because they are common fragment ions in the mass spectra of ethers and alcohols, and interesting reagent ions in chemical ionisation mass spectrometry. Although this class of compounds has been studied extensively, both theoretically and experimentally, only a few reports have dealt with the effect of increasing the size of the substituent at the oxonium ion [1–5] or bimolecular reactions of substituted oxonium ions ($R^1R^2COR^{3+}$; R^1,$R^3 \neq$ H).[6–9] The majority of the research has been concerned with unimolecular chemistry of oxonium ions,[10–33] bimolecular chemistry of the methoxy methyl cation ($CH_2OCH_3^+$),[2,7,9,34–57] and of various protonated carbonyl compounds ($R^1R^2COH^+$), see e.g.refs. 4,5,8,37,48,58–65.

Oxonium ions have two electrophilic centres, one at the α-carbon of the O-substituent and one at the carbonyl carbon. Attack of a nucleophile on the O-substituent may lead to a nucleophilic substitution (**sub**) reaction, and attack at the carbonyl carbon may initiate an addition–elimination (**ae**) reaction (Scheme 1, with ammonia as the nucleophile).

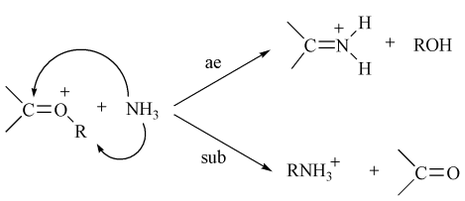

Scheme 1

Both **ae** and **sub** are important reaction types in organic chemistry, and have also been studied in the gas phase (see *e.g.* refs. 66,67 and references therein). These two reaction paths are the most common observed in reactions between $CH_2OCH_3^+$ ions and a range of nucleophiles.

We have recently investigated the effects of increasing the oxygen alkyl group in reactions between CH_2OR^+ ions and ammonia [2] (R = H, CH_3, C_2H_5, *i*-C_3H_7 and *n*-C_3H_7). In all cases both pathways mentioned above (**ae** and **sub**) were observed, and we found that the reaction rate for **ae** is only weakly dependent upon alkyl group, while the reaction rate for **sub** decreases substantially with increasingly large O-alkyl group. In the case of R = *i*-C_3H_7 and *t*-C_4H_9 [2,3] an elimination mechanism also becomes operative.

In the present work we have decided to focus on the effect of varying the alkyl group at the carbonyl carbon (Scheme 2):

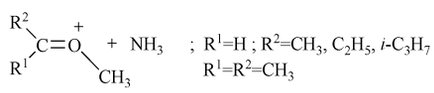

Scheme 2

From solution chemistry it is well known that increased alkyl group at the carbonyl carbon retards reactivity in most situations which involve nucleophilic attack at this atom, and the common notion is that this is due to a steric effect. It is, however, not obvious that this is also the case in the gas phase, since solvent effects may alter trends in reactivity and physical properties of molecules. In addition, it would also be of interest to see how the more remote **sub** reaction is affected by systematically changing the alkyl group at the carbonyl carbon.

Few reports exist on the bimolecular chemistry of $R^1R^2COCH_3^+$ ($R^1 \neq$H) ions in the gas phase,[6,7,9] and none of them is concerned with reactivity as a function of alkyl group. Caserio *et al.*[7,9] observed an **ae** reaction between $CH_3CHOCH_3^+$ and $CH_3OCH_2CH_2OH$, while Büchner and Grützmacher [6] found that $(CH_3)_2COCH_3^+$ is totally unreactive towards ammonia. It should also be mentioned that Williams *et al.*[68] performed a theoretical investigation and found that addition of water to unactivated carbonyl compounds slows down upon increasing the number of alkyl groups bonded to the carbonyl carbon.

Experimental and theoretical methods

Mass spectrometric experiments

The reactions were studied using an FT-ICR mass spectrometer equipped with an external EI/CI ion source (Apex 47e, Bruker Daltonics, Billerica, MA, USA). The oxonium ions ($R^1R^2COCH_3^+$) were formed by EI (70 eV) on a suitable methyl ether ($R^1R^2R^xCOCH_3$) in the external ion source. The mixture of ions produced in the process was transferred to the ICR-cell,

† Electronic supplementary information (ESI) available: proton affinities, geometries and energies of optimised structures, structures of the stationary points and a plot of experimental and RRKM $\ln(k_{ae}/k_{sub})$ against *a*-stabilisation constants. See http://www.rsc.org/suppdata/ob/b2/b209955c/

DOI: 10.1039/b209955c

which contained NH_3 at a stationary partial pressure of the order of 10^{-8}–10^{-7} mbar. All ions, except the oxonium ion of interest, were then ejected from the cell using correlated frequency sweep (CHEF).[69] An argon pulse was then introduced into the cell (peak pressure 10^{-5} mbar) to cool the ions down to ambient temperature by collisional deactivation. After a short pumping delay (3–4 s) the product and fragment ions formed in and during the cooling process were ejected from the cell by single frequency shots, in order to isolate the oxonium ion a second time. The oxonium ion was then allowed to react with ammonia before the mass spectrum was recorded. By changing the reaction delay, the time development of the system was followed, and thereby the rate constants of the individual reactions were determined. All the reaction products were isolated by using correlated sweep after an appropriate reaction time and thereby allowed to react further with ammonia. This was necessary to determine the reaction schemes unambiguously. In all cases the products showed to be unreactive towards ammonia during the timescale of interest. Due to the long reaction times and relatively high pressure of NH_3 needed in the experiments with i-$C_3H_7CHOCH_3^+$ it was on some occasions necessary to use ^{15}N labelled ammonia. Under these conditions, trace amounts of amines left over from previous experiments could be released from the walls inside the FT-ICR, and thereby be present in the gas phase during the experiments. On these occasions, the use of $^{15}NH_3$ was necessary to distinguish the wanted reaction products from protonated amines and imines formed by side reactions. In these cases we assume that isotope effects are negligible. The pressure gauge was calibrated using the $NH_3^{+\bullet} + NH_3 \longrightarrow NH_4^+ + NH_2^\bullet$ reaction with a rate constant of 2.20×10^{-9} cm^3 molecule^{-1} s^{-1}.[70] All measurements were repeated several times in different sessions to ensure long time reproducibility.

Synthesis of methyl ethers

A sample of 60% sodium hydride in mineral oil (4.0 g, 0.1 mol) was dispersed in predried DMSO and the appropriate alcohol (0.1 mol) was added during 2 h under a nitrogen atmosphere. The reaction mixture was then left stirring overnight before methyl iodide (14.2 g, 0.1 mol) in DMSO (10 ml) was added dropwise while cooling by an ice/water bath. After stirring for additional 5 h at ambient temperature the reaction mixture was poured into water and the layers were separated. Drying with MgSO4 and subsequent distillation afforded the methyl ether in 62–80% yield.

Determination of the rate constants

All the reactions observed were assumed to follow pseudo-first-order kinetics, because the neutral reactant was in great excess and held at a stationary pressure. It was shown experimentally that none of the reaction products reacted further with ammonia, so a simple kinetic procedure could be used. For a reacting system, which has two alternative reaction paths, a plot of the relative intensity of one of the products versus the other will result in a straight line. The slope of this line will then be proportional to the ratio of their rate constants. When more than two stable products are formed the same procedure can be used, but the relationship between the observed slopes and rate constants is then slightly more complicated. The individual rate constants are easily found by combining these slopes and the rate of disappearance of the reactant ion. Unfortunately, it was not possible to determine the rate constants for all the systems in the same simple manner. In the case of extremely slow reactions of i-$C_3H_7CHOCH_3^+$ there was interference with amine residues in the FT-ICR. The amines in question have higher proton affinities (PA's) than the primary products (protonated methyl amine and protonated imines), and some proton transfer was therefore observed. The assumption that the products did not react further with a neutral compound was then no longer valid. In this case the time evolution of the products was plotted, and fitted to the appropriate kinetic expression. Obviously this affects the precision of the derived kinetic parameters. The uncertainty in the absolute rate constants for $CH_3CHOCH_3^+$ and $C_2H_5CHOCH_3^+$ are about 30–35%, and about 20% for the k_{ae}/k_{sub} ratio. For i-$C_3H_7CHOCH_3^+$ the statistical uncertainties in the absolute rate constants are about 50% for k_{tot}, 110% for k_{ae} and 150% for k_{sub}. For the k_{ae}/k_{sub} ratio the uncertainty is about 120%. We want to emphasise that the large uncertainties for the i-$C_3H_7CHOCH_3^+$ system are not only due to the kinetic procedure used, but also the result of these reactions being so slow that the amount of product is close to the limit of detection.

Quantum chemical calculations

Quantum chemical calculations were carried out using the program system GAUSSIAN 98.[71] The methods used were Hartree–Fock (HF),[72] Møller–Plesset perturbation theory to second order (MP2),[73] with 3-21G and 6-31G(d,p) basis sets,[74] and the compound G2[75] method. These methods and basis-sets was chosen as to be the same used in our earlier work on oxonium ions[2,3] for the sake of comparison. All relevant critical points (reactants, transition structures, intermediates and products) of the potential energy surface were characterised by complete optimisation of the molecular geometries for HF/3-21G and MP2/6-31G(d,p), whereas the more accurate G2 method was only used in selected cases. Relative energies were calculated by including the zero-point vibrational energies (zpve) scaled by a factor of 0.9207 for the HF/3-21G and 0.9608 for the MP2/6-31G(d,p) calculations.[76] All transition states have been linked to the reactants and appropriate products by intrinsic reaction co-ordinate (IRC) calculations.[77–79] In a few cases the conformation shown for an intermediate is not that of lowest energy, but in all cases they have been linked to the corresponding lowest energy transition structure by IRC calculations. Internal energies were estimated by adding the total enthalpies of the reactants at 298 K from the G2 calculations, and then subtracting $4RT$ for redundant rotational and translational degrees of freedom and the PV terms. The result gives the amount of energy accessible for distribution between the vibrational degrees of freedom during the course of reaction.

Rice–Ramsperger–Kassel–Marcus (RRKM) reaction rate calculations[80]

The standard Beyer–Swinehart procedure was employed to calculate theoretical rate coefficients for the **ae** and **sub** reactions.[80] The scaled normal vibrational frequencies and the energy difference between the appropriate intermediate and transition structure from the MP2/6-31G(d,p) calculations were used as input. In all cases the intermediate for the **ae** reaction was found to be lowest in energy, so it was chosen as the common intermediate for the competing reactions. Rate constants were estimated at the average thermal energy. Details of the calculations (Cartesian co-ordinates, list of frequencies *etc.*) may be obtained from the authors upon request.

Results

For all the monosubstituted (R^1 = H) oxonium ions, three different ionic products were observed in the reaction with ammonia, corresponding to addition followed by elimination (**ae**), nucleophilic substitution (**sub**) and proton transfer (**pt**). A mass spectrum for the reaction between $C_2H_5CHOCH_3^+$ and NH_3 taken after an appropriate reaction time is shown in Fig. 1, and the proposed reaction scheme in Scheme 3. Both isolation experiments and the comparison of known PA values[81] (see Table S1 in the electronic supplementary information (ESI)†) showed that none of the ionic products have the capacity to transfer a proton to ammonia. The rate constants are given in

Table 1 Experimental and theoretical (RRKM) rate constants

$R^1R^2COCH_3^+ + NH_3$								
R^1	R^2	k_{ae} [a]	k_{sub} [a]	k_{pt} [a]	k_{ae}/k_{sub}	k_{pt}/k_{ae}	k_{tot} [a]	k_{ae}/k_{sub} (RRKM)
H	H	2.7	0.25	—	10.8	—	3.0	5
	CH_3	0.023	0.0088	0.60	2.6	26.1	0.63	0.6
	C_2H_5	0.016	0.0020	0.077	8.0	4.8	0.095	1.1
	i-C_3H_7	0.00023	0.000042	<0.0005	5.6	<2.4	<0.00073	3.0
CH_3	CH_3	No reactions observed					<0.0002	0.3

[a] Given in units of 10^{-10} cm^3 molecule^{-1} s^{-1}.

Table 2 Potential energies relative to the reactants for the addition–elimination reactions with MP2/6-31G(d,p). All values are given in kJ mol^{-1}

$R^1R^2COCH_3^+ + NH_3$					
R^1	R^2	*E*(INC1)	*E*(TS)	*E*(INC2)	*E*(Prod)
H	H	−178.1	−73.8	−143.6	−78.5
	CH_3	−134.2	−34.4	−117.3	−61.1
	C_2H_5	−128.7	−29.6	−111.5	−60.1
	i-C_3H_7	−129.2	−29.9 (−28.3)[a]	−146.1 (−112.7)[a]	−59.9
CH_3	CH_3	−108.7	−10.8	−108.9	−57.9

[a] Please note that the product side INC2 in the case of *i*-$C_3H_7CHOCH_3^+$ is different from the corresponding complexes found for R^2= H, CH_3 and C_2H_5 (see structures **5**, Fig. S1 (ESI)†). Separate IRC calculations show that the transition structure is topographically linked to a hydrogen bonded species (structure **5c′**). For the sake of direct comparison we have included the covalently bonded species for R^2 = *i*-C_3H_7 (**5c**) within the parenthesis, and the corresponding transition structure. This transition state differs from structure **4c** only by the conformation of the *i*-C_3H_7 group.

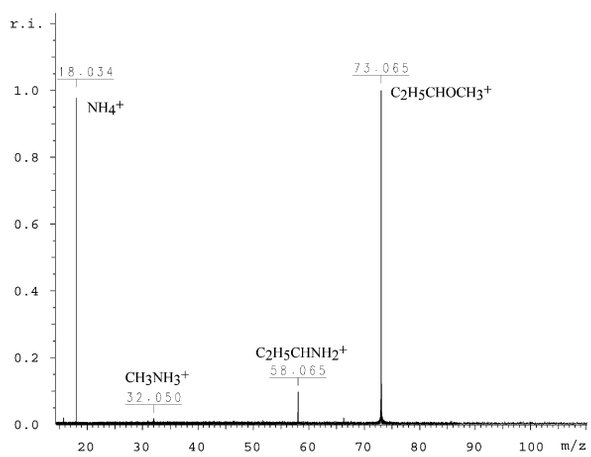

Fig. 1 Mass spectrum for the reaction between $C_2H_5CHOCH_3^+$ and NH_3, taken after 12 s at an ammonia pressure of 2.1×10^{-7} mbar.

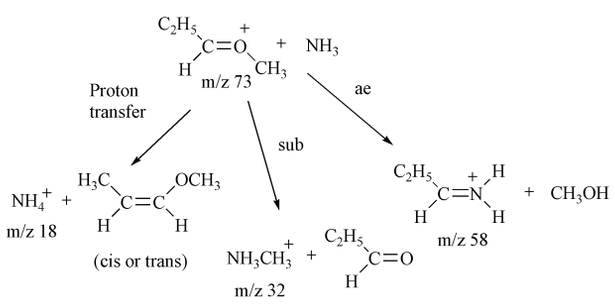

Scheme 3

Table 1, and for comparison we have also included the results for $CH_2OCH_3^+$ from our earlier investigation.[2] From Table 1 it is easily seen that the total reaction rate decreases significantly when the alkyl group increases in size. For the disubstituted oxonium ion, $(CH_3)_2COCH_3^+$, no reactions were observed within the maximum reaction time (700 s) and pressure range (2×10^{-7} mbar). This gives an upper limit to the total rate constant in the order of 2×10^{-14} cm^3 molecules^{-1} s^{-1}, in agreement with the findings of Büchner and Grützmacher.[6]

The addition–elimination reactions

The **ae** reaction is observed for all the oxonium ions, except for the dimethyl ion which is unreactive. As shown in Table 1 there is a marked drop in the reaction rate with bigger R group. The effect is most pronounced when adding the first (R^1 = H; R^2 = CH_3) and the second (R^1 = R^2 = CH_3) methyl group to the carbonyl carbon, but there is also a large drop in rate constants between $C_2H_5CHOCH_3^+$ and *i*-$C_3H_7CHOCH_3^+$.

The *ab initio* calculations show that the **ae** reaction is initiated by attack of ammonia on the carbonyl carbon leading to the first ion–neutral complex (INC1), as shown in Fig. 2 for $C_2H_5CHOCH_3^+$. The label b on the enumeration of the structures refers to R^2=C_2H_5. The reaction then proceeds through a 1,3-proton transfer from N to O, whereupon the C–O bond weakens. This leads to the formation of the second ion–neutral complex (INC2) where a protonated imine is loosely bonded to methanol, followed by dissociation of the complex into products. The relative energies are given in Table 2, and the structures in Fig. S1 with bond lengths and angles in Table S2 (ESI†). The absolute energies of the optimised points are given in Table S3 and Cartesian coordinates in Table S4 (ESI†). For comparison we have also included the results for R^1=R^2=H in the tables. From the relative energies for all relevant stationary points it is evident that the effect of changing the first H to CH_3 ($CH_2OCH_3^+$ to $CH_3CHOCH_3^+$) is more pronounced than changing the second ($CH_3CHOCH_3^+$ to $(CH_3)_2COCH_3^+$). This is the same trend as found in a theoretical study by Williams *et al.*[68] of **ae** reactions between unactivated carbonyl compounds and water; increased number of alkyl groups bonded to the carbonyl carbon increases the central barrier and makes the reactions less exothermic. When comparing bond lengths and angles in Table S2 with the data for $CH_2OCH_3^+$ (shown in the lower part of Table S2), it is seen that the effect on the transition structure of adding the first CH_3-group to the carbonyl carbon is slightly more pronounced than adding the second. The N ··· H and O ··· H distances become shorter, while the C–N and C–O bonds get longer. Interestingly, the variations are most pronounced in the C–O and O ··· H bonds, reflecting that increased size of the alkyl bonded directly to C=O affects this part of the transition structures mostly.

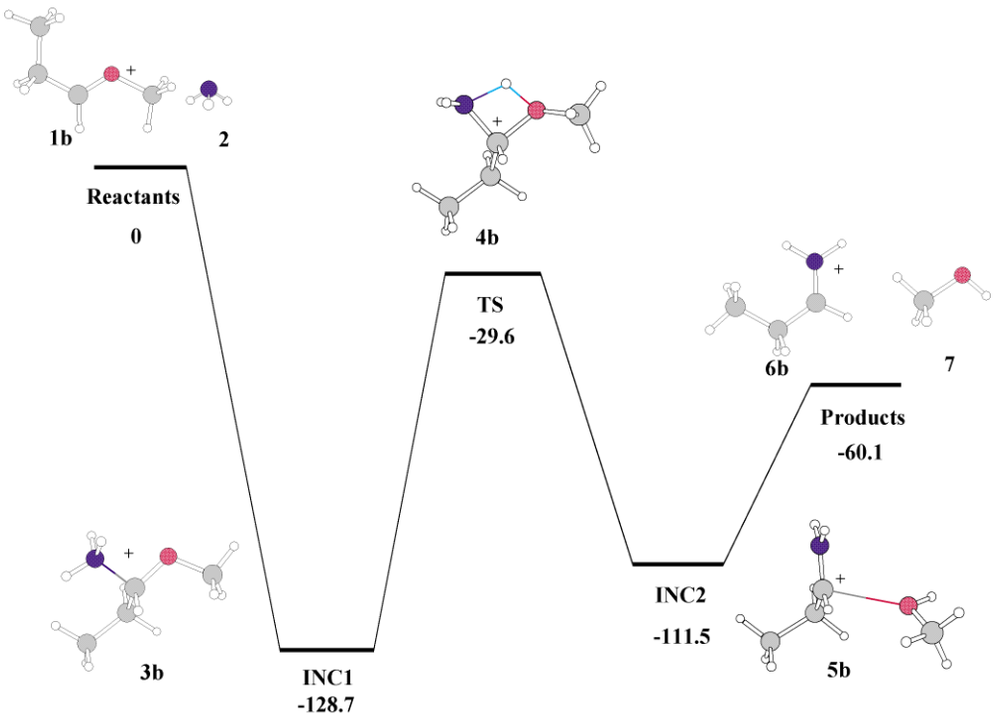

Fig. 2 MP2/6-31G(d,p) potential energy diagram for the addition–elimination reaction between $C_2H_5CHOCH_3^+$ and NH_3. All values are given in kJ mol^{-1}.

Table 3 Potential energies relative to the reactants for the substitution reactions with MP2/6-31G(d,p). All values are given in kJ mol^{-1}

$R^1R^2COCH_3^+ + NH_3$					
R^1	R^2	*E*(INC1)	*E*(TS)	*E*(INC2)	*E*(Prod)
H	H	−52.7	−38.3	−184.9	−146.8
	CH_3	−47.2	−19.0	−145.4	−100.2
	C_2H_5	−46.1	−15.6	−138.4	−92.7
	i-C_3H_7	−45.1	−12.2	−132.3	−85.7
CH_3	CH_3	−43.3	−1.1	−122.5	−72.4

When we examine the isolated oxonium ions we see the same trends as we do with the complexes; the structural differences between $CH_3CHOCH_3^+$, $C_2H_5CHOCH_3^+$ and *i*-C_3H_7-$CHOCH_3^+$ are quite small, while the differences between $CH_2OCH_3^+$, $CH_3CHOCH_3^+$ and $(CH_3)_2COCH_3^+$ are more pronounced. The oxonium ions become more carbinol like (shorter O–CH_3 and longer C–O bonds) when alkyl groups are attached to the carbonyl carbon compared to H, probably as a result of their higher ability to stabilise positive charge. Lossing[82] observed a similar trend in a study of ΔH_f of oxonium ions. The effect of replacing the first H with CH_3 directly on the carbonyl carbon in CH_2OR^+ ions (R=H, CH_3, C_2H_5) was larger than replacing the second H, while the effect of changing from CH_3 to C_2H_5 in the same position was even smaller (see Fig. 2 in ref. 82). This indicates that after the initial stabilisation by one CH_3-group at the carbonyl carbon ($CH_2OCH_3^+$ to CH_3-$CHOCH_3^+$), there is not much gained by increasing the size of the group in this position.

The substitution reactions

The **sub** reaction is observed experimentally for all the monosubstituted oxonium ions, and the rate constants follow the same trends as for the **ae** reaction (Table 1). There is a substantial drop in reactivity when adding the first (R^1 = H; R^2 = CH_3) and second (R^1 = R^2 = CH_3) methyl group to the carbonyl carbon, with the disubstituted oxonium ion again being unreactive. Moreover, the difference in rate constants between $CH_3CHOCH_3^+$ and $C_2H_5CHOCH_3^+$ is quite small compared to the difference between $C_2H_5CHOCH_3^+$ and *i*-$C_3H_7CHOCH_3^+$.

The reaction mechanism for nucleophilic substitution is illustrated in Fig. 3 for the reaction between $C_2H_5CHOCH_3^+$ and NH_3, and the calculated relative energies are given in Table 3. Ammonia attacks the methyl group, which then is transferred to ammonia upon inversion of configuration (Walden inversion). From Table 3 it is evident that increasing the alkyl group at the carbonyl carbon gives increased relative energies for all stationary points along the reaction co-ordinate. The trend is clear, but the effect is rather small, due to the fact that the alkyl substituents are remote from the reaction centre. Inspection of bond lengths and angles for the transition structures (complexes **9** in Table S2, ESI †) shows that increasingly large group leads to a situation where the transition structure is positioned later along the reaction co-ordinate (shorter N ⋯ CH_3 and longer O ⋯ CH_3), reflecting the larger methyl cation affinities of higher aldehydes and ketones.

The proton transfer reactions

Formation of NH_4^+ was observed for all the monosubstituted oxonium ions, although the signal is weak and almost drowns in the background for *i*-$C_3H_7CHOCH_3^+$. Separate isolation experiments, showed that none of the ionic reaction products ($RCHNH_2^+$ and $CH_3NH_3^+$) are able to transfer a proton to ammonia, at least not when thermalised. This is in accordance with known relative proton affinities. The observed NH_4^+ is therefore most likely a result of a direct encounter between the oxonium ion and ammonia. The origin of the proton being transferred was determined by examining the reactivity of the isotopic species $CH_3CHOCD_3^+$. The only **pt** product observed was NH_4^+, no NH_3D^+ was detected. This indicates that the proton originates solely from the carbon side of the carbonyl bond. *Ab initio* calculations of Okada *et al.*[36] have shown that there is a considerable reaction barrier for **pt** from the O-substituent in $CH_2OCH_3^+$ to NH_3. Due to poor S/N level and side reactions with amine residues in the ICR-cell (see Experimental section), it was not possible to determine a reliable rate constant for **pt** from *i*-$C_3H_7CHOCH_3^+$ to NH_3. In this case the difference between the total rate constant, k_{tot}, and $k_{ae} + k_{sub}$ was taken as

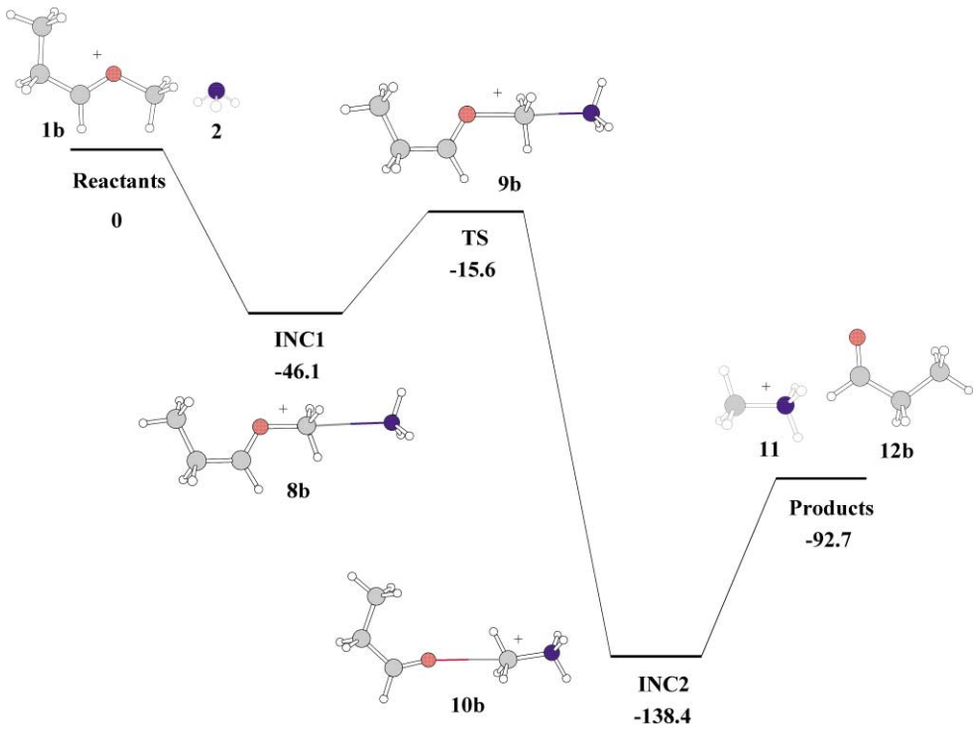

Fig. 3 MP2/6-31G(d,p) potential energy diagram for the substitution reaction between $C_2H_5CHOCH_3^+$ and NH_3. All values are given in kJ mol^{-1}.

Table 4 Potential energies relative to the reactants for the proton transfer reactions with MP2/6-31G(d,p). All values are given in kJ mol^{-1}

$R^1R^2COCH_3^+ + NH_3$					
R^1	R^2	*E*(INC1)	*E*(TS)	*E*(INC2)	*E*(Prod)
H	CH_3	−51.2	−49.4	−91.6	−3.9
	C_2H_5 (cis)	−50.0	−49.4	−97.7	+4.7
	C_2H_5 (trans)	−45.4	−44.6	−98.2	−0.7
	i-C_3H_7	−48.4	−49.8	−106.9	+1.7
CH_3	CH_3	−53.3	−36.4	−42.5	+30.2

an upper limit to the **pt** reaction. All the observed **pt** reactions are seen to be slow, and there is a drop in reactivity when the alkyl group is bigger. No reaction was observed for $(CH_3)_2COCH_3^+$.

As illustrated in Fig. 4 for the **pt** from $C_2H_5CHOCH_3^+$ to NH_3, the reaction is initiated by attack of ammonia on one of the β-hydrogens of the C-substituent, which then is transferred to ammonia forming an enol ether (**17**) and the ammonium ion (**16**). Despite the favourable low energies of all transition structures of Table 4, proton transfer is noticeably slow. The reason lies in the latter part of the reaction, since the reaction energies according to MP2/6-31G(d,p) are close to zero. The bottleneck is therefore not the central barrier since a major part of the reaction trajectories will recross the transition state and dissociate back to reactants, rather than dissociate to form products.

Discussion

As already mentioned, the aim of this work is to examine trends and to compare directly with previous work, we are confident that the MP2/6-31G(d,p) serves our purposes. However, we should not expect that this method will give highly accurate absolute energies. Since we decided not to conduct resource demanding G2 calculations for all structures involved, we find it mandatory to comment on the accuracy of the MP2/6-31G(d,p) calculations. For the analogous reactions between ammonia and CH_2OR^+ oxonium ions, we found that relative MP2/6-31G(d,p) energies of intermediates and transition structures along the **ae** and **sub** paths are underestimated by approximately 29 and 14 kJ mol^{-1}, respectively. This tendency was demonstrated by comparison with the more accurate G2 energies.[2] The results of a G2 calculation on the **ae** transition structure in the reaction between NH_3 and $(CH_3)_2COCH_3^+$ indicates exactly the same tendency. With G2 the **ae** transition structure was found to be 21 kJ mol^{-1} higher in energy than the reactants, compared to 11 kJ mol^{-1} lower in energy with MP2 (see the upper part of Table S4, ESI † for the relative G2 **ae** and **sub** transition structure energies.) This fact must be taken into consideration when we consider the quantum chemical model data of this study in greater detail.

For the **ae** reactions the relative energies of the transition structures are quite similar for the monosubstituted oxonium ions (Table 2). This is reflected in the k_{ae} rate constants for $CH_3CHOCH_3^+$ and $C_2H_5CHOCH_3^+$ (Table 1). The same is the case with the **sub** reactions (Tables 1 and 3). The reason why the rate constants for *i*-$C_3H_7CHOCH_3^+$ in both cases differ from the other monosubstituted oxonium ions is not at once evident from the MP2/6-31G(d,p) energy data. If we make the reasonable assumption that MP2/6-31G(d,p) underestimates the TS energies also in this case of R^2 = *i*-C_3H_7, the relative energies of **ae** and **sub** transition structures are at +1 and +2 kJ mol^{-1}, respectively. This would implement a quite effective barrier towards reaction, and even small changes in TS energy in this range may lead to significant changes in reaction rates. We believe that this is the reason why the k_{ae} and k_{sub} rate constants for *i*-$C_3H_7CHOCH_3^+$ are lower than for the other monosubstituted oxonium ions in this study. When viewed in light of the calculated G2 transition structure energy for the **ae** reaction (+21 kJ mol^{-1}) and the anticipated G2 transition structure energy for the **sub** reaction (+13 kJ mol^{-1}), it is also evident why $(CH_3)_2COCH_3^+$ is totally unreactive towards ammonia along these two reaction paths.

It is clear from the energies of Tables 4 and S1 why the **pt** reactions are so slow, and why the rate constants decrease with increased substitution. For all the monosubstituted oxonium ions the **pt** reactions are close to thermoneutral, and the energy requirement is seen to increase with larger alkyl group. Again, we find that even small changes in reaction energy close to the threshold may cause great variations in

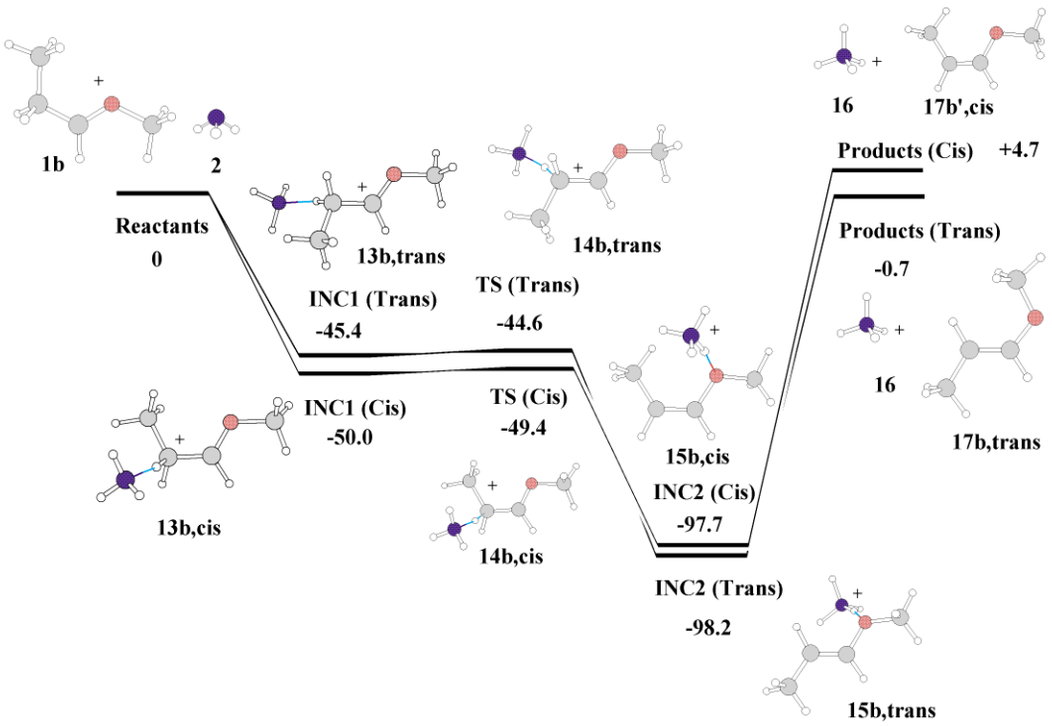

Fig. 4 MP2/6-31G(d,p) potential energy diagram for the proton transfer reaction between $C_2H_5CHOCH_3^+$ and NH_3. All values are given in kJ mol^{-1}.

reactivity, and we would expect to observe barrier crossing and re-crossing. Interestingly, we were able to discover this dynamical process. When $(CH_3)_2COCH_3^+$ was reacted with ND_3, extensive H/D-exchange was detected.

Hammett plots are often invoked to describe substituent effects in quantitative terms. There are, however, inherent problems related to the interpretation of such effects in the sense that sometimes two – and even more different constants are needed to give a comprehensive description of the influence of one substituent to various molecular properties, including reactivity. These constants (named inductive, field, resonance and steric constants) are interpreted on the basis of classical electrostatics in a quite intuitive fashion, and have usually no firm physical root, in the meaning that these named properties cannot be derived directly from the Schrödinger equation. An equally serious problem emerges from the fact that substituent constants may include unknown solvent effects.

In an effort to resolve these dilemmas and to define a basis for systematic interpretation of the inherent properties of simple gas phase molecules, we recently introduced a set of substituent constants for the most common alkyl groups.[83] These so-called *a* constants were obtained from reliable gas phase enthalpies taken from the literature, and in the first instance they reflect the Lewis acidity of the corresponding alkyl cation. However, it has become evident from experience[83,84] that the parameter is not only a measure for the ability to stabilise negative charge, but also the ability to stabilise a positive charges. This is probably related to the functional relationship between *a* and the polarisability of the group.[83] The linear dependence we found between the relative energies of the stationary points along the **ae** and **sub** reaction pathways and the *a* values for reactions between ammonia and various O-alkyl substituted oxonium ions,[2,3] made it natural to look for similar trends in the present study.

The *a* values for $CH_2OCH_3^+$, $CH_3CHOCH_3^+$, C_2H_5-$CHOCH_3^+$ and *i*-$C_3H_7CHOCH_3^+$ are as follows: 1.000(H), 0.938(CH_3), 0.915(C_2H_5), 0.895(*i*-C_3H_7). In the present study one problem had to be solved first, since no *a* constant was available for the disubstituted compound (R^1= R^2= CH_3). To overcome this, we conducted the plot shown in Fig. 5. The plot shows that the proton affinities of the homologous series of

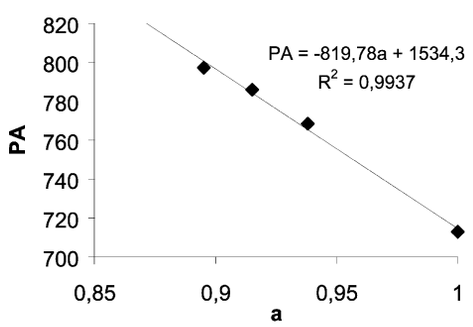

Fig. 5 Proton affinity of the relevant aldehydes and ketone plotted as a function of the *a* stabilisation constants.

aldehydes are linear in *a*. By extrapolating the straight line (R = 0.994) to the value of the proton affinity of acetone, we postulate an *a* value for the reaction of with $R^1 = R^2 = CH_3$ of *a* = 0.881. Since the *a* value of methyl is 0.938 the effect of having two methyl groups is close to the twice of having one. For the **pt** reactions the effect of R on the attacked carbon is of relevance. The substituent constants which apply for $CH_3CHOCH_3^+$, $C_2H_5CHOCH_3^+$ and *i*-$C_3H_7CHOCH_3^+$ are therefore: 1.000(H), 0.938(CH_3), and 0.881(2 × CH_3).

Fig. 6 displays the relative MP2/6-31G(d,p) energies of all stationary points (intermediates, transition structures and products) for the three reactions; **ae**, **sub** and **pt** as function of the *a*-value corresponding to the carbonyl carbon substituent. For simplicity, we have only included the values for the *trans* reaction of $C_2H_5CHOCH_3^+$ in Fig. 6c. If we exclude the $(CH_3)_2COCH_3^+$ data (the leftmost points of Fig. 6a and b) we see clear trends in the data for the **ae** and the **sub** reactions for the $R^2CHOCH_3^+$ ions. In essence the energies of all intermediate points relate to the exothermicity for the over-all reaction. We are reluctant to attribute the trend to an artefact of the moderately small wave function since the theoretical model seems to describe the experimental observations quite well, except of course the aforementioned systematic errors. We also make another interesting observation — the plots give almost straight lines, but closer examination reveals slight curvature and thereby deviation from linearity. This apparent higher

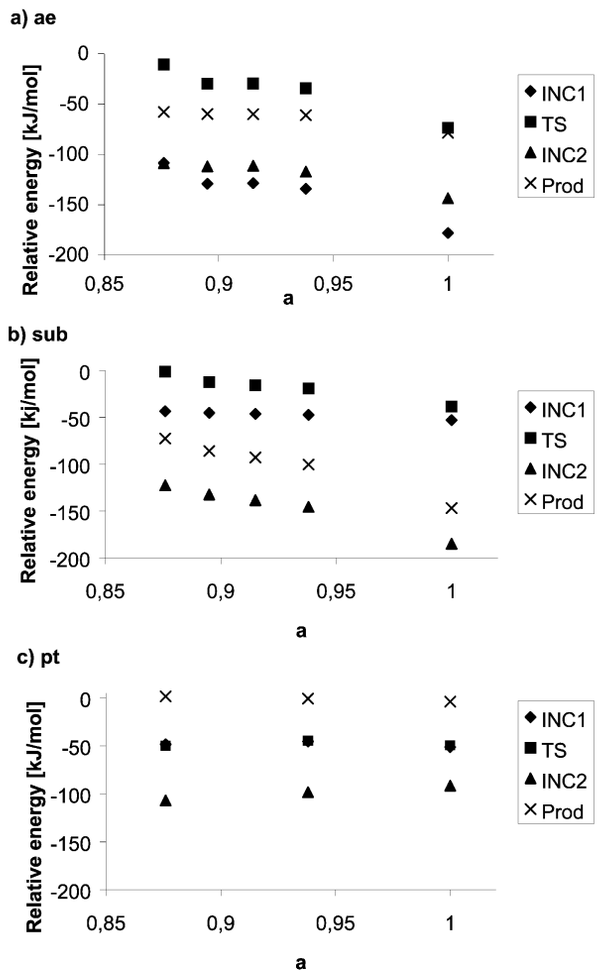

Fig. 6 Relative energies for the **ae** (a), **sub** (b) and **pt** (c) reactions plotted as a function of the *a* stabilisation constants.

order (non-linear) response is interesting, and assuming that it is not related to deficiencies in MP2/6-31G(d,p) it is somewhat different from the almost perfectly linear trend found for the previously reported reactivity of CH_2OR^+ ions.[2,3] It therefore seems that the detailed mode of transmission of the substituent effect can be slightly different depending on whether the substituent is positioned at the electropositive carbon or the electronegative oxygen. However, it is also clear that the *a* values are fully adequate descriptors of the effect and the trends are the same.

Another point should also be noted; larger substituents with smaller *a* values increase the relative energies of all stationary points along the reaction co-ordinate, in particular for the transition structure which is determining for the reactivity. A larger substituent gives rise to a less stable transition structure relative to the reactants, indicating that the effect is electronic in its nature, and that the polarizability of the alkyl group is the key issue. It is highly relevant that the trends in reactivity correlate with the Mulliken population at the carbonyl carbon, as shown in Table S5 in the ESI. † Interestingly, the Mulliken populations at the carbonyl carbon for the $CH_2OCH_3^+$, $CH_3CHOCH_3^+$ and $(CH_3)_2COCH_3^+$ series is perfectly linear in *a*. This is an important point indicating that the substituent effect is purely electronic in its nature. It is of course a matter of taste to describe this as a result of stabilization of reactants or destabilization of the transition structure. Since reactivity is so well explained via the single electronic parameter *a*, we tend to describe this as a purely electronic effect, rather than applying the popular, but rather poorly defined term "steric effect". In any instance, both "steric" and "electronic" effects have been implemented by different workers to explain the same trends in the properties of carbonyl compounds.[85] Moreover, separate considerations by us have shown that polarizability volumes (classical electrostatic effect)[83] as well as steric bulk (in terms of Exner's substituent factors[86]) increase smoothly upon decreasing *a*-value. The most fruitful point of view is therefore that "steric" or "electronic" are completely entangled. In terms of "steric" effects, the reaction centre is sufficiently remote to exclude significant steric interaction for **sub**, while the reaction centre for the **ae** mechanism is directly adjacent to the substituent. A comparison between Fig. 6a and b shows that there is no obvious qualitative difference in the curves for the two.

Finally, we would like to make a comparison between the experimental and theoretical data. For all the monosubstituted oxonium ions investigated **ae** dominates over **sub**, although to a different extent. This seems to be the norm when $CH_2OCH_3^+$ ions are reacted with nucleophiles that contain an hydrogen adjacent to the nucleophilic centre. In all cases the transition structure for the **sub** reaction is highest in energy, followed by **ae** and then **pt**. This alone indicates the same reactivity order between **ae** and **sub** as observed experimentally. But the complication of having three competing reactions hinders a direct quantitative comparison of the isolated rate constants of Table 1 and the barriers of Tables 2, 3 and 4. On the other hand, a limited comparison between the **ae** and **sub** data could provide a meaningful way to assess the accuracy of the relative theoretical transition structure energies of the two reactions. In order to do obtain theoretical estimates of the rates coefficients, we first performed RRKM calculations based on the quantum chemical data (to include all statistical factors due to internal rotation and frequencies of vibration), and then plotted both the theoretical and the experimental $\ln(k_{ae}/k_{sub})$ ratios against the corresponding *a*-values (Fig. S2, ESI †). The data could indicate a systematic tendency since in all cases the experimental ratio is larger than that estimated on the basis of the quantum chemical calculations. This does not necessarily have to mean that the MP2/6-31G(d,p) systematically underestimates the barrier of **ae** compared to **sub**, although this is what the G2-calculations indicates for the CH_2OR^+/NH_3 system.[2] We have observed that the rate *vs.* energy curves for **sub** is steeper than the **ae** curves, reflecting the tighter transition structure of the latter. Since the reaction barrier is higher for **sub** this means that the curves cross at quite low energies. Taking the uncertainty in the internal energy distribution of the reacting molecules into account, it therefore becomes impossible to rationalise the deviations on a quantitative basis. A simple statistical analysis shows that the difference in the experimental and theoretical ratios on an average is 1.3 with an estimated standard deviation of 0.6 (Fig. S2, ESI †). We consider the standard deviation to be at the limits of experimental error, so we can not make an exact statement on the magnitude of a possible non-systematic component to the deviation between theory and experiment.

Conclusion

The effect of increasingly large alkyl group on the reactions between methyl oxonium ions and ammonia is most pronounced when substituting CH_3 for H directly on the carbonyl carbon. The difference in reactivity between $CH_3CHOCH_3^+$ and $C_2H_5CHOCH_3^+$ is smaller, except for the **pt** reaction, and in line with the *ab initio* results. The differences between $C_2H_5CHOCH_3^+$ and *i*-$C_3H_7CHOCH_3^+$ are more pronounced, although there are only small differences in central barriers and reaction energies. The **pt** reactions are slightly endothermic so the same argument applies here. The most dramatic example is provided for $(CH_3)_2COCH_3^+$. It is concluded that the observed substituent effects are well described with the *a* values introduced by us previously, and at a very fundamental level the trends are described as due to a purely electronic effect.

Acknowledgements

The authors wish to thank the Norwegian Research Council for computer time and Mr Vidar Bjørnstad for the synthesis of the ethers.

References

1 K. B. Astin, *Tetrahedron Lett.*, 1980, **21**, 3713–3716.
2 L. Bache-Andreassen and E. Uggerud, *Int. J. Mass Spectrom.*, 2000, **195/196**, 171–184.
3 L. Bache-Andreassen and E. Uggerud, *Int. J. Mass Spectrom.*, 2001, **210/211**, 459–468.
4 C. H. Chu and J. J. Ho, *J. Phys. Chem.*, 1995, **99**, 16590–16596.
5 C. H. Chu and J. J. Ho, *J. Am. Chem. Soc.*, 1995, **117**, 1076–1082.
6 M. Büchner and H.-F. Grützmacher, *Int. J. Mass Spectrom.*, 2000, **199**, 141–154.
7 J. K. Pau, J. K. Kim and M. C. Caserio, *J. Chem. Soc., Chem. Commun.*, 1974, 120–121.
8 J. K. Pau, M. C. Caserio and J. K. Kim, *J. Am. Chem. Soc.*, 1978, **100**, 3831–3837.
9 J. K. Pau, J. K. Kim and M. C. Caserio, *J. Am. Chem. Soc.*, 1978, **100**, 3838–3846.
10 R. D. Bowen, *Org. Mass Spectrom.*, 1993, **28**, 1577–1595.
11 H. E. Audier, G. Bouchoux, T. B. McMahon, A. Milliet and T. Vulpius, *Org. Mass Spectrom.*, 1994, **29**, 176–185.
12 F. Bernardi, I. G. Csizmadia, H. B. Schlegel and S. Wolfe, *Can. J. Chem.*, 1975, **53**, 1144–1153.
13 R. D. Bowen, D. H. Williams, G. Hvistendahl and J.R. Kalman, *Org. Mass Spectrom.*, 1978, **13**, 721–728.
14 R. D. Bowen and A. G. Harrison, *Org. Mass Spectrom.*, 1981, **16**, 159–166.
15 G. Bouchoux, F. Penaud-Berruyer, H. E. Audier, P. Mourgues and J. Tortajada, *J. Mass Spectrom.*, 1997, **32**, 188–200.
16 R. D. Bowen, A. W. Colburn and P. J. Derrick, *J. Chem. Soc. Perkin Trans. 2*, 1991, 147–151.
17 A. J. Chalk and L. Radom, *J. Am. Chem. Soc.*, 1998, **120**, 8430–8437.
18 Y.-P. Tu and J. L. Holmes, *J. Am. Soc. Mass Spectrom.*, 1999, **10**, 386–392.
19 G. Hvistendahl and E. Uggerud, *Org. Mass Spectrom.*, 1985, **20**, 541–542.
20 G. Hvistendahl and E. Uggerud, *Org. Mass Spectrom.*, 1991, **26**, 67–73.
21 T. J. Mead and D. H. Williams, *J. Chem. Soc. Perkin Trans. 2*, 1972, 876–882.
22 R. H. Nobes, W. R. Rodwell, W. J. Bouma and L. Radom, *J. Am. Chem. Soc.*, 1981, **103**, 1913–1922.
23 R. H. Nobes and L. Radom, *Org. Mass Spectrom.*, 1984, **19**, 385–393.
24 D. Farcasiu and J. A. Horsley, *J. Am. Chem. Soc.*, 1980, **102**, 4906–4911.
25 J. V. Headly and A. G. Harrison, *Can. J. Chem.*, 1985, **63**, 609–618.
26 D. J. McAdoo and C. E. Hudson, *Int. J. Mass Spectrom. Ion Processes*, 1989, **88**, 133–146.
27 H. Schwartz and D. Stahl, *Int. J. Mass Spectrom. Ion Processes*, 1980, **36**, 285–289.
28 J. Tortajada and H. E. Audier, *Org. Mass Spectrom.*, 1991, **26**, 913–914.
29 J.L. Holmes, R. T. B. Rye and J. K. Terlouw, *Org. Mass Spectrom.*, 1979, **14**, 606–608.
30 R. D. Bowen and P. J. Derrick, *Org. Mass Spectrom.*, 1993, **28**, 1197–1209.
31 D. H. Williams and R. D. Bowen, *J. Am. Chem. Soc.*, 1977, **99**, 3192–3194.
32 G. Hvistendahl and D. H. Williams, *J. Am. Chem. Soc.*, 1975, **97**, 3097–3101.
33 R. D. Bowen and D. H. Williams, *J. Am. Chem. Soc.*, 1978, **100**, 7454–7459.
34 H. E. Audier and T. B. McMahon, *J. Mass Spectrom.*, 1997, **32**, 201–208.
35 M. C. Caserio and J. K. Kim, *J. Org. Chem.*, 1982, **47**, 2940–2944.
36 S. Okada, Y. Abe, S. Taniguchi and S. Yamabe, *J. Am. Chem. Soc.*, 1987, **109**, 295–300.
37 M. T. Kinter and M. M. Bursey, *J. Am. Chem. Soc.*, 1986, **108**, 1797–1801.
38 R. van Doorn and N. M. M. Nibbering, *Org. Mass Spectrom.*, 1978, **13**, 527–534.
39 P. F. Wilson, M. J. McEwan and M. Meot-Ner, *Int. J. Mass Spectrom. Ion Processes*, 1994, **132**, 149–152.
40 E. J. Alvarez and J. S. Brodbelt, *J. Mass Spectrom.*, 1996, **31**, 901–907.
41 T. D. McCarley and J. Brodbelt, *Anal. Chem.*, 1993, **65**, 2380–2388.
42 T. Keough, *Anal. Chem.*, 1982, **54**, 2540–2547.
43 J. Brodbelt, C. Liou and T. Donovan, *Anal. Chem.*, 1991, **63**, 1205–1209.
44 E. S. Eichmann and J. S. Brodbelt, *J. Am. Soc. Mass Spectrom.*, 1993, **4**, 230–241.
45 E. S. Eichmann and J. S. Brodbelt, *J. Am. Soc. Mass Spectrom.*, 1993, **4**, 97–105.
46 T. D. McCarly and J. Brodbelt, *J. Am. Soc. Mass Spectrom.*, 1993, **4**, 352–361.
47 M. A. Freitas and R. A. J. O'Hair, *Int. J. Mass Spectrom. Ion Processes*, 1998, **175**, 107–122.
48 J. L. Beauchamp and R. C. Dunbar, *J. Am. Chem. Soc.*, 1970, **92**, 1477–1485.
49 R. A. J. O'Hair, M. A. Freitas, S. Gronert, J. A. R. Schmidt and T. D. Williams, *J. Org. Chem.*, 1995, **60**, 1990–1998.
50 A. Matsumoto, S. Okada, S. Taniguchi and T. Hayakawa, *Bull. Chem. Soc. Jpn.*, 1975, **48**, 3387–3388.
51 J. K. Kim, J. Bonicamp and M. C. Caserio, *J. Org. Chem.*, 1981, **46**, 4230–4236.
52 J. K. Pau, M. B. Ruggera, J. K. Kim and M. C. Caserio, *J. Am. Chem. Soc.*, 1978, **100**, 4242–4248.
53 J. K. Kim, J. Bonicamp and M. C. Caserio, *J. Org. Chem.*, 1981, **46**, 4236–4242.
54 M. A. Freitas, R. A. J. O'Hair and T. D. Willimas, *J. Org. Chem.*, 1997, **62**, 6112–6120.
55 E. S. Eichmann and J. S. Brodbelt, *Org. Mass Spectrom.*, 1993, **28**, 737–744.
56 G. F. Bauerle, B. J. Hall, N. V. Tran and J. S. Brodbelt, *J. Am. Soc. Mass Spectrom.*, 1996, **7**, 250–260.
57 G. van der Rest, G. Bouchoux, H. E. Audier and T. B. McMahon, *Eur. Mass Spectrom.*, 1998, **4**, 339–347.
58 M. Pykäläinen, A. Vainiotalo, T. Pakkanen and P. Vainiotalo, *J. Mass Spectrom.*, 1996, **31**, 716–726.
59 Y. Hoppilliard and G. Bouchoux, *Int. J. Mass Spectrom. Ion Processes*, 1987, **75**, 1–14.
60 I. H. Williams, G. M. Maggiora and R. L. Schowen, *J. Am. Chem. Soc.*, 1980, **102**, 7831–7839.
61 G. van der Rest, P. Morgues, J. Fossey and H. E. Audier, *Int. J. Mass Spectrom. Ion Processes*, 1997, **160**, 107–115.
62 C. H. Chu and J. J. Ho, *J. Phys. Chem.*, 1995, **99**, 1151–1155.
63 S. Prabhakar and M. Vairamani, *Mass Spectrom. Rev.*, 1997, **16**, 259–281.
64 E. Uggerud, *J. Chem. Soc. Perkin Trans. 2*, 1996, 1915–1920.
65 R. A. J. O'Hair and S. Gronert, *Int. J. Mass Spectrom.*, 2000, **195/196**, 303–317.
66 S. Gronert, *Chem. Rev.*, 2001, **101**, 329–360.
67 J. K. Laerdahl and E. Uggerud, *Int. J. Mass Spectrom.*, 2002, **214**, 277–314.
68 I. H. Williams, D. Sprangler, G. M. Maggiora and R. L. Schowen, *J. Am. Chem. Soc.*, 1985, **107**, 7717–7723.
69 L. J. de Koning, N. M. M. Nibbering, S. L. van Orden and F. H. Laukien, *Int. J. Mass Spectrom. Ion Processes*, 1997, **165/166**, 209–219.
70 Y. Ikezoe, S. Matsuoka, M. Takebe and A. Viggiano, *Gas Phase Ion-Molecule Reaction Rate Constants Through 1986*, Maruzen, Tokyo, 1987.
71 M. J. Frisch, G. W. Trucks, H. B. Schlegel, G. E. Scuseria, M. A. Robb, J. R. Cheeseman, V. G. Zakrzewski, J. A. Montgomery, Jr., R. E. Stratmann, J. C. Burant, S. Dapprich, J. M. Millam, A. D. Daniels, K. N. Kudin, M. C. Strain, O. Farkas, J. Tomasi, V. Barone, M. Cossi, R. Cammi, B. Mennucci, C. Pomelli, C. Adamo, S. Clifford, J. Ochterski, G. A. Petersson, P. Y. Ayala, Q. Cui, K. Morokuma, D. K. Malick, A. D. Rabuck, K. Raghavachari, J. B. Foresman, J. Cioslowski, J. V. Ortiz, B. B. Stefanov, G. Liu, A. Liashenko, P. Piskorz, I. Komaromi, R. Gomperts, R. L. Martin, D. J. Fox, T. Keith, M. A. Al-Laham, C. Y. Peng, A. Nanayakkara, C. Gonzalez, M. Challacombe, P. M. W. Gill, B. G. Johnson, W. Chen, M. W. Wong, J. L. Andres, M. Head-Gordon, E. S. Replogle and J. A. Pople, GAUSSIAN 98, Gaussian, Inc., Pittsburgh, PA, 1998.
72 C. C. J. Roothaan, *Rev. Mod. Phys.*, 1951, **23**, 69–89.
73 C. Møller and M. S. Plesset, *Phys. Rev.*, 1934, **46**, 618–622.
74 M. J. Frisch, J. A. Pople and J. S. Binkley, *J. Chem. Phys.*, 1984, **80**, 3265–3269.
75 L. A. Curtiss, K. Raghavachari, G. W. Trucks and J. A. Pople, *J. Chem. Phys.*, 1991, **94**, 7221–7230.
76 A. P. Scott and L. Radom, *J. Phys. Chem.*, 1996, **100**, 16502–16513.
77 C. Gonzales and H. B. Schlegel, *J. Phys. Chem.*, 1990, **94**, 5523–5527.

78 C. Gonzales and H. B. Schlegel, *J. Chem. Phys.*, 1989, **90**, 2154–2161.
79 K. Fukui, *J. Phys. Chem.*, 1970, **74**, 4161–4163.
80 R. G. Gilbert and S. C. Smith, *Theory of Unimolecular and Recombination Reactions*, Blackwell Scientific Publications, Oxford, 1990.
81 E. P. Hunter and S. G. Lias, in *NIST Chemistry WebBook, NIST Standard Reference Database Number 69*, eds P. J. Linstrom and W. G. Mallard, 2001, National Institute of Standards and Technology, Gaithersburg MD, http://webbook.nist.gov/m.
82 F. P. Lossing, *J. Am. Chem. Soc.*, 1977, **99**, 7526–7530.
83 E. Uggerud, *Eur. Mass Spectrom.*, 2000, **6**, 131–134.
84 E. Uggerud, *Modern Mass Spectrometry*, ed. C. Schalley, Springer Verlag, Heidelberg, accepted for publication.
85 H. Homan, M. Herreros, R. Notario, J. L. M. Abboud, M. Esseffar, H. Mo, M. Yanez, C. Foces-Foces, A. Ramos-Gallardo, M. Martinez-Ripoll, A. Vegas, M. T. Molina, J. Casanovas, P. Jimenez, M. V. Roux and C. Turrion, *J. Org. Chem.*, 1997, **62**, 8503–8512.
86 O. Exner, *J. Phys. Org. Chem.*, 1999, **12**, 265–274.